Microseismic hypocenter location using nonlinear optimization

Joe Wong

ABSTRACT

Reduced arrival times from microseismograms caused by hydraulic fracturing and recorded by borehole or surface arrays of geophones can be modeled assuming a layered-earth velocity model. These reduced times are independent of t_0, the unknown clock time at which a microseismic event occurs. Ray-tracing through a layered-earth velocity model can be used to calculate arrival times from a hypocenter to the geophone arrays. Assuming that we know the velocity model, the receiver coordinates, and observed arrival times, we can use a nonlinear optimization method similar to the Levenberg-Marquardt algorithm to find the microseismic source coordinates if the array of geophones spans a sufficient solid angle relative to the source.

The location of hypocenters requires that the velocities in the layered-earth model be known. In real-world microseismic surveys, arrival times observed from a perforation shot in the treatment well are used to calibrate the velocity values. If the perforation shot location, the geophone coordinates, and layer depths are known, the model velocities can be ascertained. Synthetic arrival-time data created by ray-tracing were used in a simulation of velocity calibration. An objective function equal to the RMS misfit between synthetic observed and calculated arrival times was created. The required velocity values were found by using search schemes such as the genetic algorithm and pattern search to minimize the arrival time misfit. For this simulation, the search method performed better than the modified LM technique and the genetic algorithm.

INTRODUCTION

Hydraulic fracturing is a widely used procedure used to increase the permeability and production rates in tight oil and gas reservoirs. Fluids and proppants are pumped at high-pressure into a treatment well and applied to a specific zone isolated top and bottom by packers. The high pressure creates cracks in the rock which propagate away from the well for some distance and in some direction into the producing formation. Knowing the geometry in 3D space of such hydraulic fractures is important for planning the development of the reservoir.

A way of mapping the hydraulic fracture is to use the seismic waves generated by the micro-earthquakes that occur as the rock is being fractured. A microseism is located at a hypocenter that coincides with the point of fracturing. When the resulting seismic waves are detected and recorded as seismograms by an array of geophones, either in one or more observation wells or on the ground surface, the first-arrival times can be used to estimate the 3D coordinates of the hypocenter. As the hydraulic fracture develops over time, more and more microseismic events are recorded, and mapping all the associated hypocenters is equivalent to mapping the fracture. This report deals with the issue of finding the coordinates of the microseismic hypocenter given a set of arrival times from a geophone array.

NONLINEAR OPTIMIZATION

Assume a microseismic event occurring at a hypocenter with coordinates (x_s, y_s, z_s). Ray-tracing can be used to calculate the first-arrival times $t_{cal}(i)$ for an array of n geophones with coordinates $(x_g(i), y_g(i), z_g(i))$. The underlying velocity model for the ray-tracing is either a homogeneous or a horizontally layered earth. The observed first-arrival times on field seismograms are $t_{obs}(i)$. The hypocenter mapping problem is to estimate coordinates (x_s, y_s, z_s), given the known geophone coordinates $(x_g(i), y_g(i), z_g(i))$, the velocity model, and the observed arrival times $t_{obs}(i)$. This is a classic geophysical inverse problem solved by nonlinear optimization schemes. Using ray-tracing through an appropriate velocity model to calculate arrival times, a scheme for solving the problem involves these steps:

1. Define an objective function equal to the variance between n observed arrival times and n calculated arrival times:

$$f(x_s, y_s, z_s) = \sum_{i=1}^{n}[t_{obs}(i) - t_{cal}(i)]^2 .$$

2. Set values for the experimental error ***exp_err***, and the maximum number of iterations ***iter_max***. Set the iteration counter ***iter*** to 1.
3. Make an initial guess for the coordinates ***(x_s, y_s, z_s)***.
4. Calculate ***$t_{cal}(i)$*** for i=1 to n, by ray-tracing through the velocity model.
5. Find the residuals ***$t_{obs}(i)$ - $t_{cal}(i)$***.
6. Calculate ***rms_err*** = the root-mean-square value of ***$t_{obs}(i)$ - $t_{cal}(i)$***.
7. Go to Step 15 if ***rms_err*** is less than ***exp_err***.
8. Use local gradient of the objective function and the residuals to estimate corrections $(\Delta x_s, \Delta y_s, \Delta z_s)$.
9. Update the coordinates $(x_s = x_s + \Delta x_s, y_s = y_s + \Delta y_s, z_s = z_s + \Delta z_s)$.
10. Calculate ***$t_{cal}(i)$*** and ***rms_err***.
11. Go to 15 if ***rms_err*** is less than ***exp_err***.
12. If the current ***rms_err*** is greater than the last ***rms_err***, then

    (a) set λ =.5 and ***iter2*** =1;
    (b) reset $(x_s, y_s, z_s) = (x_s = x_s - \Delta x_s, y_s = y_s - \Delta y_s, z_s = z_s - \Delta z_s)$;
    (c) decrease $(\Delta x_s, \Delta y_s, \Delta z_s) = \lambda (\Delta x_s, \Delta y_s, \Delta z_s)$;
    (d) update the coordinates $(x_s = x_s + \Delta x_s, y_s = y_s + \Delta y_s, z_s = z_s + \Delta z_s)$;
    (e) calculate ***$t_{cal}(i)$*** and ***rms_err*** ;
    (f) go to step 15 if ***rms_err*** is less than ***exp_err***;
    (g) go to (b) if rms_error has increased;
    (h) set ***iter2*** = ***iter2***+1;
    (i) go to (a) if ***iter2*** <= 5.

13. Increment ***iter*** = ***iter*** +1.
14. If ***iter*** > ***iter_max*** go to step 3.
15. Stop.

The key to nonlinear optimization is to estimate *effective* values for the corrections (Δx_s, Δy_s, Δz_s). By effective, we mean that the corrections must decrease the residuals $t_{obs}(i) - t_{cal}(i)$. The literature is replete with detailed descriptions of how to do this; see Press (1992) for a list of references. Here, we use the singular-value decomposition (SVD) algorithm published by Golub and Rensch (1977) for step 8 to estimate the direction of a linear gradient. Step 12 finds an appropriate length for the correction vector, based on ideas given by Levenberg (1944) and Marquardt (1977). Our modified Levenberg-Marquardt (LM) inversion scheme has been implemented in MATLAB code.

Like other numeric minimization algorithms, the modified LM algorithm is an iterative procedure. To start a minimization, the user has to provide an initial guess for the parameter vector. The convergence to a global minimum may or may not be successful, depending on the initial guess values, and on the number of local minima, saddle points, inflection points, etc., in the objective function. At such points, the gradient is zero. If the model parameters happen to lie at or near a zero-gradient point, the corrections are also zero or near zero, and the iterative process becomes trapped at such points. In such a situation, the global minimum will not be found.

TESTING ON SYNTHETIC FIRST-ARRIVAL TIMES

Since the actual time of occurrence t_0 of a microseismic event is unknown, this is an extra parameter that must be found if we want to use true first-arrival times as the basis for the inversion scheme. We instead use the reduced arrival times $t_{obs}(i) - min(t_{obs}(i))$ and $t_{cal}(i) - min(t_{cal}(i))$ as the input data to the algorithm. This simple adjustment means that arrival-time moveouts rather than absolute arrival times are the basis for locating the hypocenter, eliminating the need to know the event time t_0. The moveouts must be large enough so that they exceed any time-picking errors. They will contain sufficient geometric information for locating the hypocenter if the angles subtended by the geophone arrays relative to the source span a range of ±20 degrees or more.

RESULTS

Inverting synthetic first-arrival times from surface arrays

Figure 1 is a section view showing a layered-earth velocity model with a prototypical array of geophones on the surface. The geometry in cylindrical coordinates is radially symmetric about the subsurface microseismic source. Assuming P-wave velocities, ray-tracing from the source to the geophone array gives a set of first-arrival times as a function of radial distance from the source. Interpolation then can be used to find the arrival time to any surface geophone with coordinates (x_g, y_g, z_g=0) after determining its radial distance from the source. This procedure for finding arrival times through any non-uniform velocity structure is known as the shooting method.

Figure 2 shows an array of 36 geophones located on the surface of a layered earth. The geophones spacing is 50m, and the array spans distances of about 250 meters in both the x and y directions. The array is approximately centered about the treatment well. A microseismic hypocenter located in the vicinity of the well at a depth of 600m is shown in green. For testing purposes in this report, we have assumed a very simple surface array with a small number of geophones. In a real-world monitoring situation, hundred

of geophones would be deployed, either along lines radiating from the treatment well or on a rectangular grid (Chambers et al., 2008; Lakings et al., 2006). The shooting method was used to generate a set of "observed" arrival times t_{obs} assuming the velocity structure in Figure 1. We then assumed that the source coordinates are unknown, attempted to estimated them from the "observed" times through inversion.

Table 1. Summary of modified LM inversion results for surface array data.

Iteration	x_s	y_s	z_s	RMS time difference
Initial guess	100	-155	900	6.31ms
17	21.6	-35.7m	731.0m	1.10ms
30	12.3m	-.5m	613.3	0.05ms
True values	10m	0m	600m	0m

Figure 3 shows the results of nonlinear optimization after 10 iterations of the Marquardt-Levenberg algorithm. The blue dots are the observed reduced arrival times. The red dots are the calculated reduced times for an initial guess for the source coordinates. The yellow dots show the calculated reduced times after 17 iterations of the algorithm. Figure 4 show the reduced times after 30 iterations; here, the yellow dots coincide with the blue dots, i.e., the final reduced times match the observed reduced times almost exactly. Table I summarizes the results of the inversion process, and shows that after 30 iterations, the inverted hypocenter coordinates were almost identical to the true coordinates.

Inverting synthetic first-arrival times from well-located geophones

The left panel of Figure 5 shows ray-tracing through the layered-earth velocity model from a microseismic source at a depth of 600m to an array of 36 geophones located in a vertical observation well about 450m to the right of a treatment well. The associated arrival times are plotted on the right panel.

For an array in a single observation well, travel times alone cannot give the horizontal coordinates (x_s, y_s) for source, but they can yield the cylindrical coordinates (r_s, z_s) where r_s is the radial distance from the observation well. In order to get the coordinates (x_s, y_s), we must have three component geophones, and use the x- and y-components with hodogram analysis to get azimuth angles to the source from the geophones. Combining the azimuths with r_s then gives estimates for (x_s, y_s). Details for hodogram/azimuth analysis can be found in Han et al. (2009). The current discussion is limited to finding (r_s, z_s) using inversion of first-arrival times through a layered-earth velocity structure.

Table 2 lists the results of applying the modified LM method to invert for a hypocenter located at $(x_s, y_s, z_s) = (0, 0, 600m)$ with arrival times observed at 36 geophones in a vertical observation well located at r=520m.

Although the modified LM inversion method successfully locates hypocenter coordinates, the method suffers from issues common to all gradient-based optimization

routines. The inversion can get trapped in local minima far from the desired true minimum. If in addition the objective function exhibits "data valleys", saddle points, and inflection points (all of which are characterized by zero or non-zero gradients), the corrections to the parameters at such points are very small, and movement away from such points is very slow or nonexistent. Even in our problem, which involves optimizing only two parameters, we have encountered unsatisfactory performance. Whether or not the method leads the hypocenter coordinates to converge to the desired location depends very much on the initial guess, on the particular way and sequence that the coordinate corrections are made, and on how we determine the amplitudes of the corrections.

Table 2. Summary of modified LM inversion results for well array data.

Iteration	r_s	x_s	z_s	RMS time difference
Initial guess	540m	-20	700	3.14ms
30	581m	-61	640m	1.13ms
200	513.5m	6.5m	606m	0.19ms
True values	520m	0	600	0

To illustrate the problem of near-zero gradients, we have used a "brute-force" mapping of the RMS fit error as a function of the two variables r_s and z_s (the radial distance and depth coordinates in a cylindrical coordinate system). Figure 7 is a contour plot of the RMS fit error showing a long narrow "data valley". In such cases, gradient methods can be very slow in finding the global minimum (Press, 1992). Experimental errors associated with the observed arrival times may cause a complete failure to converge to the global minimum. It should be noted that, for real-world digital microseismograms sampled at 0.25ms, uncertainties even in high-quality time picks would be no less than 0.5ms, and would be much higher if the seismograms are noisy.

Figure 8 is an expanded view of the contour map of RMS fit error. If our observed arrival times are such that we have an experimental error of 0.4ms, then any coordinate pair that falls within the 0.4ms contour (the cyan-coloured band) is a valid candidate for the hypocenter location. Thus, for observed arrival times with an expected uncertainty of 0.4ms, r_s is located with an uncertainty of about ±20m, while z_s is located with an uncertainty of about ±4m. These correspond to the major and minor axes of the cyan-coloured elliptical zones. If the experimental error is 1.0ms (corresponding to the yellow-coloured band), the r_s and z_s uncertainties increase to about ±50m and ±10m, respectively. These uncertainties in source coordinates depend strongly on the angles in the source-geophone configuration. Figure 7 and 8 are specific for the given velocity model and geophone array.

VELOCITY CALIBRATION USING SEARCH METHODS

Accurate determination of the hypocenter coordinates (x_s, y_s, z_s) using arrival times on microseismograms requires an accurate velocity model. A suitable velocity model is usually found from P and S velocity well-logging. The model may be refined in a

calibration step, by fixing layer boundaries at or near observed geological interfaces, and allowing the layer velocities to be found by inversion of perforation shot arrival times.

In the discussion on hypocenter location, it was pointed out that gradient-based optimization methods such as the Levenberg-Marquardt algorithm can be easily trapped in local minima even when only two variables (r_s, z_s) are to be found. In calibrating a layered-earth velocity model, more than two variables (i.e., velocities) are involved. This increases the likelihood for the existence of more local minima, saddle points, or long narrow data valleys. Trying to use a gradient method to find a global minimum in such cases tends to be a frustrating experience.

Instead, we can take advantage of sophisticated global search techniques such as the genetic algorithm (GA) or pattern search (PS). Descriptions for the GA and PS methods can be found in the literature (Torczon, 1997; Vose, 1999; Kolda et al., 2003; articles in wikipedia.org). Both algorithms are available in the utility program *optimtool* bundled in the MATLAB (2009) optimization toolbox. The user must provide a suitable objective function to be minimized. The function must be parameterized by an input vector of variables to be found. The advantages of these direct search techniques are:

- They are much less prone to being trapped in local minima.

- They require no calculation of partial derivatives of the objective function.

- Available implementations of the algorithms are easy to use.

Using the velocity model shown on Figure 6(a) and the arrival times on Figure 6(b), we simulated velocity calibration using arrival times from a perforation shot. We knew the source and geophone locations, the (synthetic) observed arrival times from the perforation shot, and the depths of the layer boundaries. We needed to find the velocity values within the layers. We used the shooting method to calculate model arrival times as a function of the input velocity values. We assumed that the layer boundaries were fixed and known through geophysical well logs. We created an objective function whose parameters were the layer velocities, and whose output was the RMS difference between calculated arrival times and observed arrival times.

We first attempted to find the correct velocity values with the modified LM method. This effort was unsatisfactory, as the inversion was prone to being trapped in local minima, and the solution did not converge quickly to the known velocity values. Performance was highly dependent on the starting values for the velocities. We then applied the GA and pattern search techniques to find [v_1, v_2, v_3, v_4] values that globally minimized the objective function.

Genetic algorithm search for velocity values

We selected the GA option in the MATLAB *optimtool* utility to minimize our objective function. To accelerate the search, reasonable lower and upper bounds for the velocities [v_1, v_2, v_3, v_4] were set at [1000, 2000, 2000, 2000] and [1000, 6000, 6000, 6000] m/s. Since the overburden velocity played no role in determining arrival times for this particular source-receiver geometry, we fixed it by setting its lower and upper bounds

at 1000m/s. The program returned velocity values that approached the global minimum within a user-determined small tolerance.

Table 3 shows the results of a specific run of the GA search. After 69 generations, during which there were 1380 evaluation of the objective function, the returned velocity values for the four layers were 1000, 3961, 3551, and 4997m/s. These were very close to the true velocity values. The minimum RMS time difference for 20 members of the last generation was .0414ms, and the mean RMS time difference for the 20 members was .0440ms. Figure 9 shows the velocity profiles after the generations listed on Table 3; Figure 10 plots and compares the corresponding calculated and observed arrival times.

Table 3. Genetics algorithm for calibrating model velocities (m/s) with well array data.

Generation	v_1	v_2	v_3	v_4	RMS error (ms)
Initial guess	1000	2000	2000	2000	31.8
10	1000	2005	3001	3116	29.43
20	1000	2000	4029	4087	11.03
30	1000	3480	3133	4472	9.14
69	1000	3961	3551	4997	.0414
True values	1000	4000	3500	5000	0

The velocities found by several separate trials of GA were very close to the exact values, and the calculated reduced times match the observed reduced times almost exactly. It should be noted that, since GA updates current best fit parameters in a semi-random fashion, the number of generations needed to reduce the fir error to an acceptable value changes from trial to trial. On Table 1, the 69 generations to reduce the fit error to the very low value of .0414ms are atypical. More typical are 90 to 100 generations, with 1800 to 2000 evaluations of the objective function, to produce a fit error of about 0.3ms.

Pattern search for velocity values

Pattern search (PS) was also used to find the velocities for the simulated calibration problem. As with GA, the number of iterations and evaluations of the objective function required to reduce the fit error to acceptable levels varied from trial to trial. However, PS performed more efficiently than GA, taking only about 1/10 the number of objective function evaluations to produce smaller fit errors. PS performed well even if the initial guess for the velocities were far from the true values. The method converged to the true values regardless of whether the lower or the upper bounds were used as starting values. Table 4 summarizes the results of four PS trials.

Bland and Hogan (2005) used PS to locate hypocenters by ray-tracing in a 3D velocity field. The ray-tracing was done using a fast marching method to solve the eikonal equation for travel times. Speed limitations in their ray-tracing procedure restricted their investigation to a 3D cube of 20 cells per dimension.

Table 4. Pattern search for calibrating model velocities (m/s) with well array data. The numbers between the parentheses in the last column are the number of objective function evaluations.

Iterations	v_1	v_2	v_3	v_4	RMS error (ms)
Initial guess	1000	2000	2000	2000	69.4
10	1000	5952	2000	5476	4.312 (16)
20	1000	3482	3976	4982	0.474 (58)
40	1000	4007	3544	4982	0.127 (148)
55	1000	3995	3513	4997	0.018 (220)
True values	1000	4000	3500	5000	0

SUMMARY AND CONCLUSIONS

Inversion of first-arrival times for locating microseismic hypocenters is not effective unless the angles subtended by both surface and well-located geophone arrays (relative to the microseismic source) are large enough to yield significant arrival time moveout. More specifically, the difference between the minimum and maximum arrival times for an array must be on the order of tens of milliseconds. The inversion scheme can be set up to use reduced travel times (i.e., arrival times minus the minimum arrival time), so that the unknown event time t_0 is eliminated from consideration. Our tests involving synthetic data show that inversion using a modified Levenberg-Marquardt algorithm often works well for data from both surface and borehole arrays over a layered earth, yielding accurate hypocenter coordinates (x_s, y_s, z_s). However, the algorithm is prone to getting trapped in local minima, and it converges very slowly in regions of the objective function with near-zer0 gradients. The performance is also dependent on the choice of starting parameter values: the closer the starting values are to the true values, the faster and more likely is the convergence to the global minimum.

The unreliable performance of gradient techniques for nonlinear optimization motivated us to investigate direct search methods, namely, the genetic algorithm (GA) and pattern search (PS). We used these techniques to calibrate a layered-earth velocity model to fit perforation shot arrival times. In this case, the arrival times as well as the source and geophone locations are known, and we must find the velocities in the layered earth model that will give calculated arrival times that match the observed arrival times. Because we anticipated that there may be many location minima and inflection points in an objective function that depends on several velocities, we applied both genetics algorithm (GA) and pattern search methods to determine the global minimum. We took advantage of the accessibility of these algorithms in the *optimtool* utility bundled in the MATLAB (2009) optimization toolkit. Both techniques were successful in finding the correct velocities in a test model, but the pattern search technique was faster and more efficient.

Based on our experience, we concluded that pattern search likely is the best choice for both microseismic hypocenter location and velocity calibration.

ACKNOWLEDGEMENTS

REFERENCES

Bland, H.C., and Hogan C., 2005. A hypocenter location method for microseismicity in complex regions: CREWES Research Report 17, 18.1-18.14.

Chambers, K., Brandsberg-Dahl, S., Kendall, J.M., and Rueda, J., 2008. Testing the ability of surface arrays to locate microseismicity: 78th Ann. Int. Meeting, SEG Expanded Abstracts, 1436-1439.

Han, L., Wong, J., and Bancroft, J.C., 2009. Microseismic hypocenter location: CREWES Report **21**, this volume.

Kolda, T.G., Lewis, R.M., and Torczon, V., 2003. Optimization by direct search: new perspectives on some classical and modern methods: Soc. for Indus. and Appl. Mathematics, **45**, 385-482.

Lakings, J.D., Duncan, P.M., Neale, C., and Theiner, T., 2006. Surface based microseismic monitoring of a hydraulic fracture well stimulation in the Barnett shale: 76th Ann. Int. Meeting, SEG Expanded Abstracts, 605-607.

Levenberg, K., 1944. A method for the solution of certain nonlinear problems in least squares: The Quarterly of Applied Mathematics, **2**, 164–168.

Marquardt, D, 1963. An algorithm for least-squares estimation of nonlinear parameters: SIAM Journal on Applied Mathematics, **11**, pp. 431–441.

Press, W.H., 1992. Numerical recipes in FORTRAN: the art of scientific computing: Cambridge University Press.

Torczon, V., 1997. On the convergence of pattern search algorithms: SIAM Jour. on Optimization: **7**, 1-25.

Whitley, D., 1994. A genetic algorithm tutorial: Statistics and Computing, **4**, 65-85.
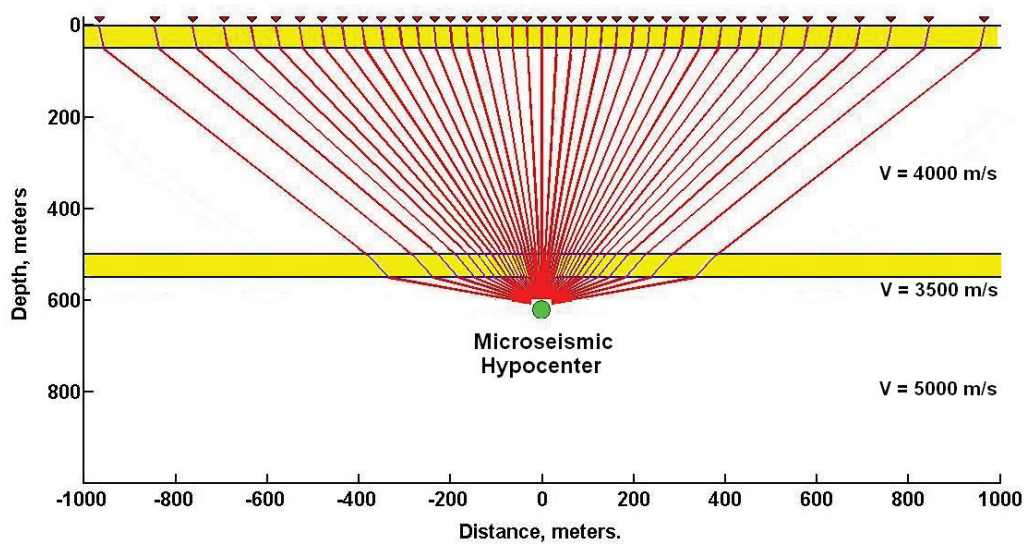
Fig 1: Section view of a microseism propagating into a surface array of geophones. Low-velocity zones are shown in yellow; the overburden velocity is 1000m/s. The geometry is radially symmetric.
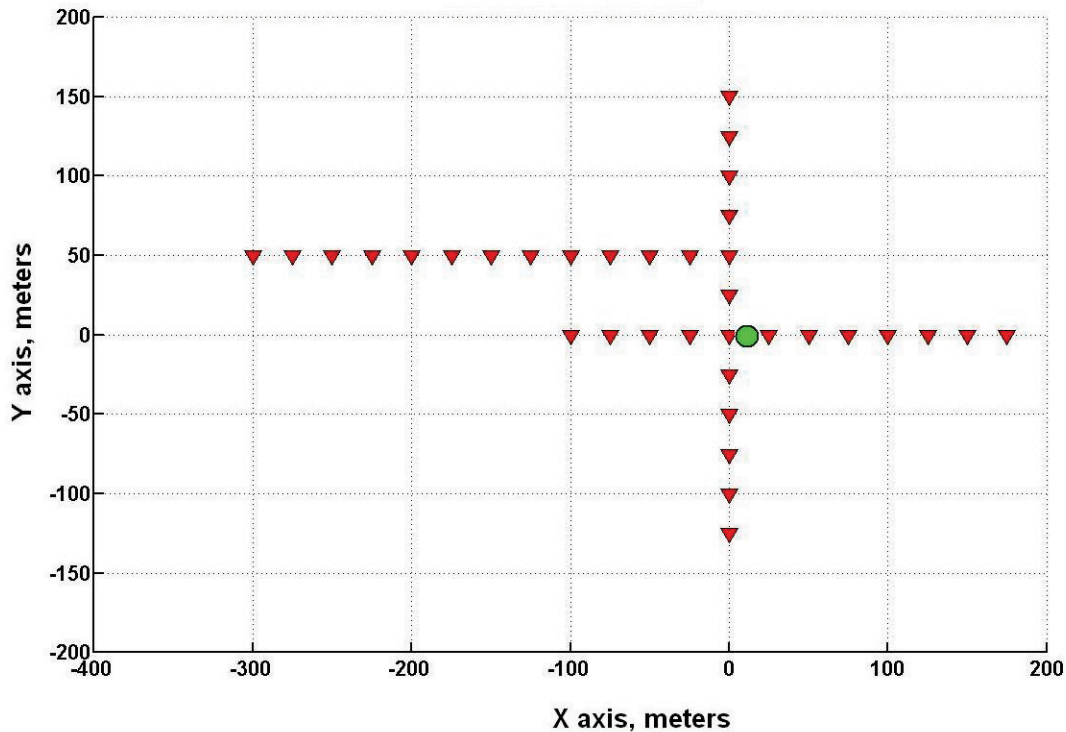

Fig 2: Plan view of a surface array of geophones for microseismic monitoring. The subsurface microseismic source, located at a depth of 600m, is shown in green.
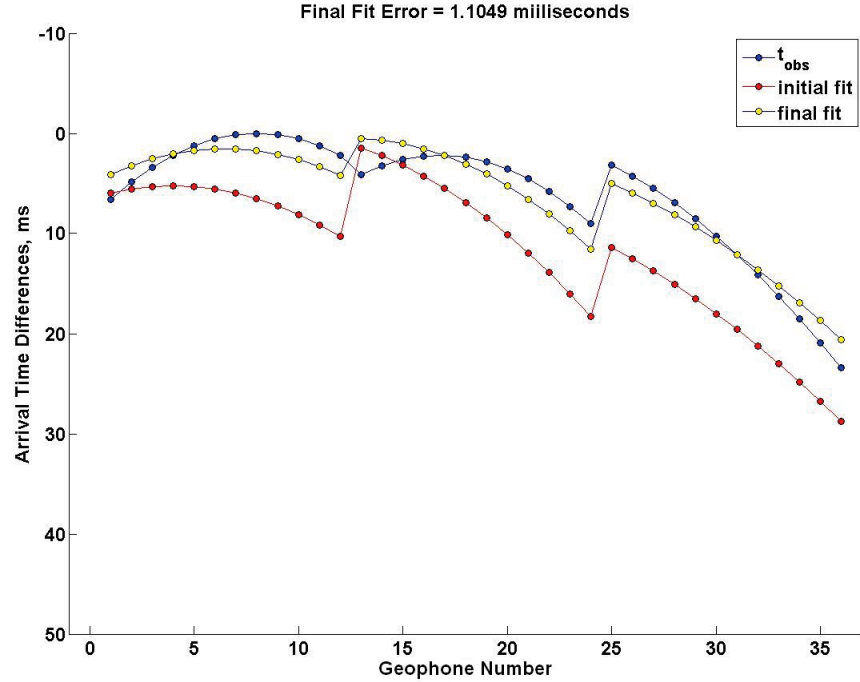
Fig. 3: Reduced arrival times for the surface array. Blue dots are the observed times; red dots are calculated times from the initial guess for the source coordinates; yellow dots are calculated times from relocated source coordinates after 17 iterations of the modified LM optimization routine. The RMS difference between observed times and current calculated times is 1.10ms.
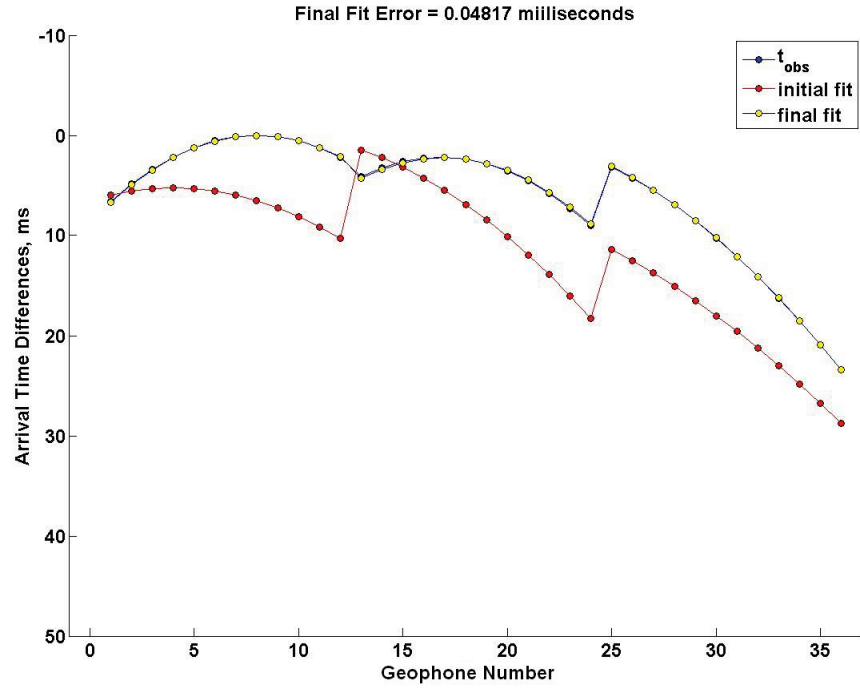
Fig. 4: Reduced arrival times for the surface array after 30 iterations of the modified LM optimization routine. The RMS difference between observed times and current calculated times is about 0.05ms.
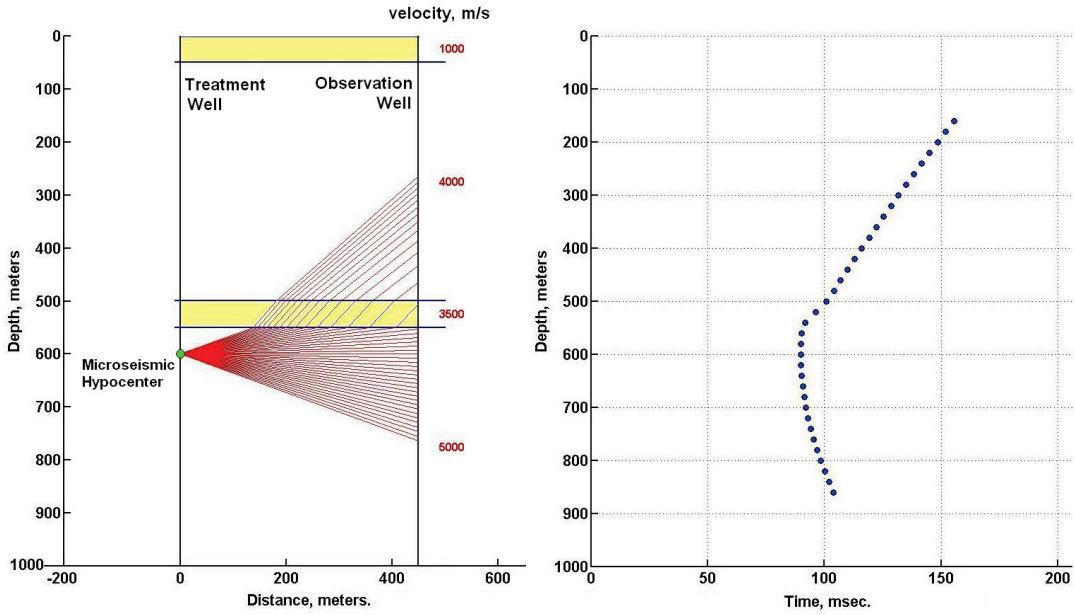
Fig 5: Left panel: ray-tracing and first arrival times between a microseismic source and an array of geophones in a vertical borehole. Note the refraction through the low-velocity zone. Right panel: the associated arrival times.
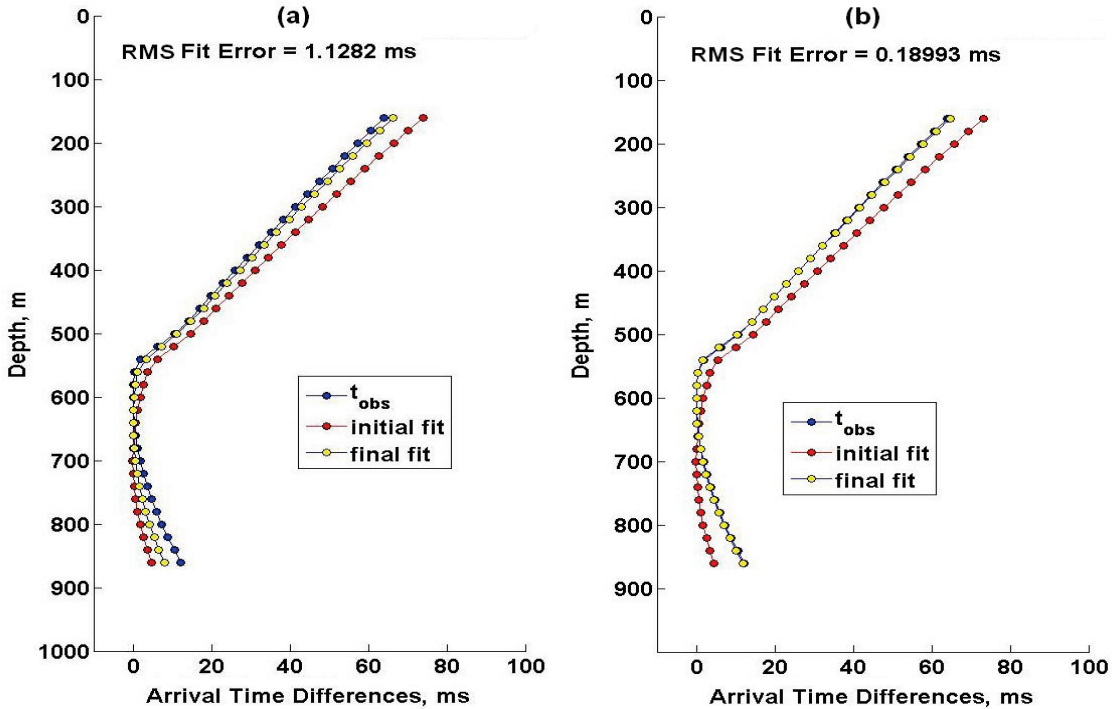

Fig. 6: Reduced arrival times for the borehole array after (a) 30, and (b) 200 iterations of the modified LM optimization routine. The RMS difference between observed times and the calculated times after 200 iterations is about 0.19ms.
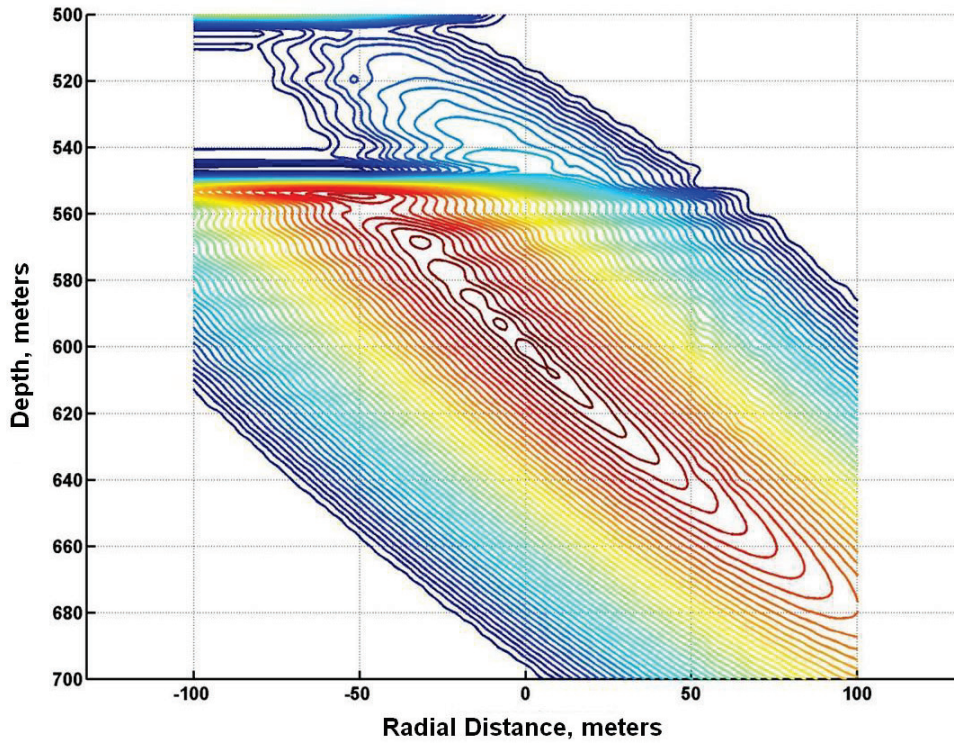
Fig. 7: RMS error between observed reduced times and calculated reduced times for different assumed coordinates of the microseismic source. Contour levels are separated by .2ms.
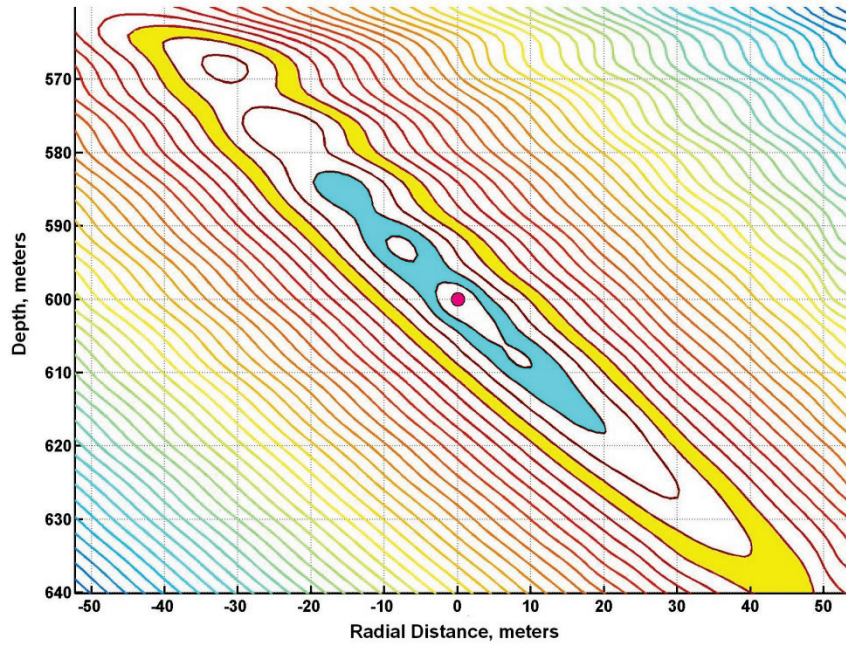

Fig. 8: Expanded view of RMS error between reduced observed times and calculated times for different assumed coordinates of the microseismic source. The red dot is the true hypocenter location, where the RMS error is zero. The yellow band represents errors between 0.8ms and 1.0ms; the cyan band represents errors between 0.2ms and 0.4ms.
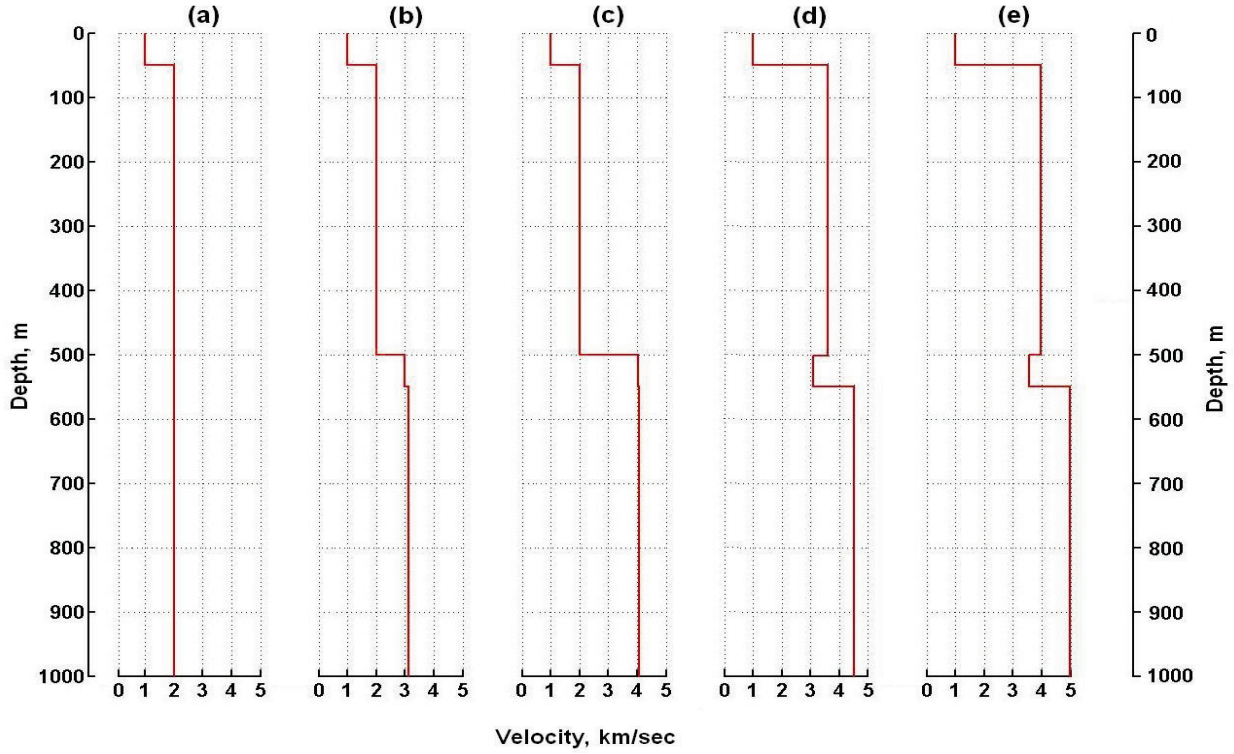
Fig. 9: Velocity profiles from genetics algorithm search after (a) 1 generation (starting values); (b) 10 generations; (c) 20 generations; (d) 30 generations; (e) 69 generations (final values).
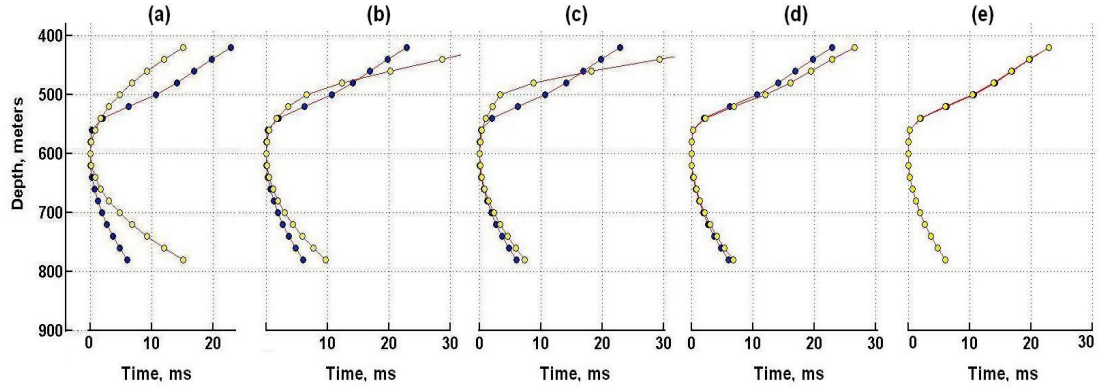

Fig. 10: First-arrival time fits for the velocity profiles in Figure 9. Blue dots are the reduced observed times from a calibration shot. Yellow dots are reduced calculated times for the velocity profiles in Figure 9 after (a) 1 generation (starting values); (b) 10 generations; (c) 20 generations; (d) 30 generations; (e) 69 generations (final values).